Nuclear Instruments and Methods in Physics Research A 606 (2009) 589–597

Contents lists available at ScienceDirect

Nuclear Instruments and Methods in Physics Research A

journal homepage: www.elsevier.com/locate/nima

A new simulation package to model detector systems with fragmentation reactions and ion separators: Application to the LYCCA-0 system

M.J. Taylor [a,*], M.A. Bentley [a], D. Rudolph [b], C. Fahlander [b], P. Golubev [b], R. Hoischen [b], P. Reiter [c], J. Gerl [d], M. Górska [d]

[a] Department of Physics, University of York, Heslington, York YO10 5DD, UK
[b] Department of Physics, Lund University, 22100 Lund, Sweden
[c] Institut für Kernphysik, Universität zu Köln, 50937 Köln, Germany
[d] Gesellschaft für Schwerionenforschung (GSI), Planckstrasse 1, 64291 Darmstadt, Germany

ARTICLE INFO

Article history:
Received 27 November 2008
Received in revised form
1 May 2009
Accepted 3 May 2009
Available online 13 May 2009

Keywords:
Monte-Carlo
Geant4
Mocadi
Simulation
Fragmentation
LYCCA

ABSTRACT

A Monte-Carlo simulation package has been developed to model the response of a detector system for ion identification used in conjunction with ion separators following nuclear reactions. The simulation is written predominantly using the GEANT4 framework but utilises the ion transport code MOCADI for accurate separator and reaction modelling. A novel MOCADI–GEANT4 interface has been developed to utilise the parameter file output option of MOCADI as an event generator for the GEANT4 detector simulation. Test simulation results have been compared with experimental data and excellent agreement was observed. The simulation has successfully been used to model a new particle detection system prototype (Lund-York-Cologne CAlorimeter (LYCCA)-0) and validate a method of ion identification using energy and time-of-flight with this system.

1. Introduction

As experimental nuclear structure studies extend away from stable nuclei and towards the proton and neutron drip-lines, accessing more exotic isotopes becomes extremely difficult with stable beams and targets. Therefore the future of nuclear structure physics will need radioactive ion beams (RIBs) to produce the nuclei of interest. One method of RIB production is projectile fragmentation which is currently used by many accelerator facilities worldwide with new facilities and upgrades at existing laboratories planned to extend the range and quality of RIBs. The nuclei to be studied will often be produced with small cross-sections, thus the clean identification of all (non-light particle) reaction products is essential. Spectroscopic studies in particular will require accurate ion identification in order to ascertain the origin of detected nuclear de-excitation radiation. Many techniques and devices are currently employed to determine the charge and mass of reaction products including electromagnetic spectrometers and solid state detector telescopes. New systems to identify and select low cross-section reaction channels are becoming increasingly complex, hence it is desirable to not only be able to simulate the detector system to be utilised but also the whole measurement environment including the reaction process. Moreover, the added complexity and cost of new systems means that simulating detector response becomes a crucial stage in their design.

Various software packages and codes exist to simulate nuclear reactions such as projectile fragmentation, transfer and Coulomb excitation as well as the passage of ions through magnetic separators. For example, reaction codes such as ABRABLA [1] and EPAX2 [2] can calculate cross-sections and yields for fragmentation reactions and GOSIA [3] and CLX [4] calculate similar quantities for Coulomb excitation. MOCADI [5] and LISE++ [6,7] incorporate EPAX2 to not only model the reaction process but also the passage of the produced ions through a magnetic separator. There also exists software to model particle detector geometries and their response to ion implantation and radiation. Software frameworks such as GEANT4 [8] and MCNP [9] allow the user to define and model detector systems by tracking particles and radiation through sensitive detectors. Although all of these software packages are state-of-the-art and have been rigorously tested and improved, some over many years, there does not exist a software package to completely simulate detector response, nuclear reactions at relativistic energies and magnetic separators to produce simulated data in a format analogous to that collected during a real experiment. Ideally, one would utilise some of these

* Corresponding author. Tel.: +44 1904 432245; fax: +44 1904 432214.
E-mail address: mjt502@york.ac.uk (M.J. Taylor).

0168-9002/$ - see front matter © 2009 Elsevier B.V. All rights reserved.
doi:10.1016/j.nima.2009.05.003

tried and tested programs to build a complete experimental simulation package but difficulties arise at the interfaces between the codes. A new simulation package has therefore been created which incorporates some of the aforementioned programs along with newly developed interfaces and modules.

2. Simulation overview

Fig. 1 shows a basic block diagram of the complete simulation package which can be considered to consist of three main stages with interfaces between each stage. The first stage is primarily concerned with the generation of RIBs via projectile fragmentation reactions. The reaction between a stable beam and target is modelled and the resulting reaction products enter a device to separate and select a particular fragment. The final part of stage 1 is to model a secondary reaction involving the newly produced RIB to produce and/or excite the nuclei to be studied.

The second stage of the simulation is concerned with the tracking of the nuclei from stage 1 onto and through a virtual particle detector system. Physics processes are invoked to determine the results of interactions between the nuclei and the sensitive detector material. The third and final stage takes the simulated detector signals, digitises and stores them in a suitable format for later analysis. Simple algorithms can also be applied at this stage, the results of which can be histogrammed along with the raw detector signals.

3. Software choices

The Monte-Carlo simulation framework GEANT4 was chosen to model the particle detector elements for stage 2. GEANT4 has been used extensively by the high energy physics community for detector simulations but its capabilities are now being realised by nuclear physicists. A GEANT4 user application can not only model the response of particle detectors but also model a number of nuclear reactions and has the ability to track the passage of charged particles through magnetic fields. Using GEANT4 to simulate an ion separation device or nuclear reactions (in stage 1) is not a trivial task and is also rather unnecessary as many such tried and tested applications already exist (see Section 1). Therefore, to simulate the passage of ions through an ion separator in stage 1 the program MOCADI was chosen.

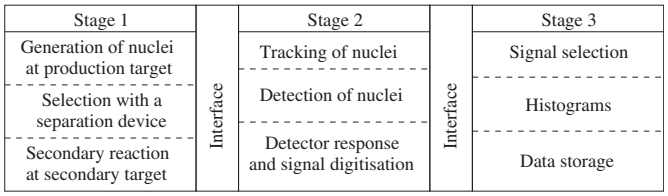

Fig. 1. A basic schematic diagram detailing the three main stages that comprise the complete simulation package.

MOCADI allows the user to simulate a range of separators by defining the corresponding magnets, collimators, slits and tracking detector materials. Fragmentation reactions incorporating the Goldhaber momentum distribution [10] can also be modelled with MOCADI with an option to output parameters describing the ions at certain points in the separator setup to a text file.

The data analysis package ROOT [11] is the software chosen with which to analyse the simulation results for stage 3. The ROOT package contains a powerful data compression feature for the storage of large correlated data sets. ROOT is written in C++, as is the GEANT4 framework and therefore can easily be linked with a GEANT4 application negating the need for an interface between stages 2 and 3 (Fig. 1). All of this makes ROOT an ideal choice for the histogramming, storage and analysis of the simulated data.

Fig. 2 shows a more detailed schematic diagram of the simulation package highlighting the three stages involved and the need for only a single interface (between stages 1 and 2) due to the outlined software choices.

4. Stage 1: MOCADI simulations

One advantage of using an external program such as MOCADI to model a nuclear reaction and produce a file parameterising the reaction products is that the file can be used repeatedly for different detector geometries. This maintains a level of consistency when optimising or investigating different detector configurations and also reduces the simulation running time as new reaction products need not be generated after each detector modification. MOCADI is used to simulate both the primary and the secondary reactions, that is, the RIB production and the production/excitation of the nuclei of interest. A MOCADI input file is produced which describes all of the magnet elements, collimating slits and tracking detector materials for the ion separator being simulated as well as any reaction targets to be used. A primary beam with, energy, spatial distribution and divergence parameters is defined along with the number of primary beam particles to be generated. After the primary

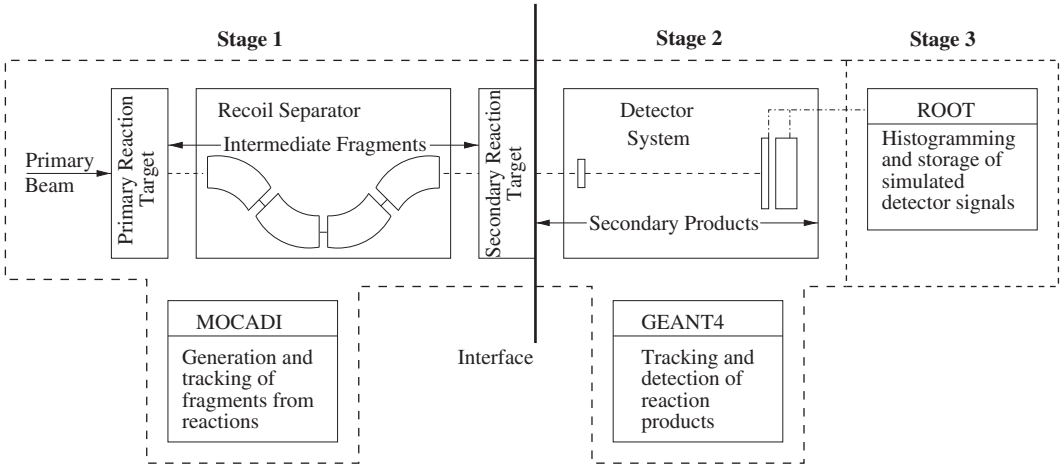

Fig. 2. A detailed schematic diagram of the simulation package highlighting the software choices and their roles for each stage of the process.

reaction between the beam and the first reaction target, the ion optics are optimised for a particular intermediate fragment (see Fig. 2). The intermediate fragments that emerge from the separator can then impinge on a second reaction target. To produce a range of secondary reaction products, MOCADI needs to be run multiple times, once for each required ion type. For each generated primary beam particle, the parameters describing each intermediate and/or secondary ion are written to a file at every user defined 'save point' that the ion successfully reaches in the virtual separator setup. These save points can be used to evaluate quantities such as position and energy loss in the separator tracking detectors. After stage 1 of the simulation, the generated parameter files need to be collated and modified in order to be used in stage 2.

5. MOCADI–GEANT4 interface

The parameter files produced by MOCADI (stage 1) are used to generate the ions in the GEANT4 application (stage 2) that will interact with the detector system. As MOCADI was never developed with this goal in mind, some modifications to the parameter files need to be performed to produce files suitable for stage 2. This is the interface stage shown in Fig. 2 and is a multi-step process utilising scripts and programs developed using Perl and C++. Perl is a powerful scripting language with many file manipulation commands and C++ is a multipurpose, high-level object-oriented programming language in which GEANT4 is written, making them both the languages of choice.

As mentioned in Section 4, MOCADI has to be run multiple times if a range of nuclei are to be produced in the secondary reaction. This is performed with a Perl script which substitutes new A and Z values in the input file, from a pre-determined list, for each required secondary reaction product. After each substitution, the script executes MOCADI and appends an integer to each outputted text file. Once all of the parameter files have been generated another Perl script is used to separate the data into two files, one containing all of the parameters describing the intermediate fragments at each save point and another for the secondary reaction products. This step is required as only the secondary products are tracked by the GEANT4 application. As MOCADI outputs the parameters for every surviving ion, production cross-sections need to be applied to reflect the relative yields. The EPAX2 production cross-sections are listed for each ion in the corresponding output files. These are automatically retrieved and then applied to the secondary products listed in the parameter file by a C++ program. During the cross-section application process the correlations between the intermediate and secondary ions are preserved; any intermediate fragments that do not reach the second reaction target are discarded. Once all of the modifications have been applied, two parameter files exist describing the correlated intermediate and secondary ions, which are then used as input files for the next stage of the simulation.

6. Stage 2: GEANT4 application

Stage two of the simulation package consists of an application written predominantly using the GEANT4 framework. Within the code, each detector geometry is defined as well as the physics processes that govern the ion interactions with the sensitive detector regions. A new C++ class has been developed, *ReadMocadiEvent*, to read the parameter files and pass the values to the GEANT4 application event-by-event. For each event, the application uses the GEANT4 *particleGun* class to create an ion, at a particular spatial position, with mass, charge, energy and trajectory, all defined by the read parameters. After creation, the ion is tracked onto and through the complete detection system geometry until it either leaves the specified 'world volume' or comes to rest inside a detector medium. A *Digitisation* module, for signal processing, is defined in the application for each detector type. The module outputs digitised detector signals, for example, deposited energy, position and time. The *Digitisation* method also applies a Gaussian distribution, of specified width, to each signal in order to simulate the time and/or energy resolution of the detector and associated electronics. The application has a graphical interface which allows the user to change the detection system position and various detector resolution widths interactively without the need to recompile the code.

7. Stage 3: ROOT analysis

The third and final stage of the simulation is the analysis, histogramming and storage of the simulated detector signals. ROOT histogram creation methods are called directly by the GEANT4 application and the histograms are filled on an event-by-event basis. The *Analysis* module can also be used to perform basic signal analysis, for example, a time-of-flight calculation from the difference between detector time signals. All of the user calculated quantities and raw detector signals are stored in a ROOT Tree object for post-simulation data analysis.

8. Simulation test case

8.1. Detector: LYCCA-0

LYCCA-0 is the first prototype of LYCCA (Lund-York-Cologne CAlorimeter) [12], a device to identify nuclei following reactions involving exotic radioactive beams. LYCCA will be used in the HISPEC (High resolution In-flight SPECtroscopy) [13] programme as part of the NuStAR (Nuclear Structure Astrophysics and Reactions) [14] collaboration at the international facility FAIR (Facility for Anti-proton and Ion Research) [15]. The system will consist of separate detector modules which can be positioned in a variety of geometries and will use an energy loss (ΔE), residual energy (E_r) and time-of-flight (TOF) method to identify nuclei following the secondary reaction. Each LYCCA-0 module has a $6 \times 6\,\mathrm{cm}^2$, 300 μm thick, position sensitive DSSSD (Doubled-Sided Silicon-Strip Detector) for accurate particle tracking and charge identification through energy loss; 5 mm behind each DSSSD resides one or more CsI(Tl) scintillation detectors to record the residual energy as the particles come to rest. Two types of CsI detector will be used, $5.4 \times 5.4\,\mathrm{cm}^2$, 1 cm thick and $19 \times 19\,\mathrm{mm}^2$, 11 mm thick. The $19 \times 19\,\mathrm{mm}^2$ square detectors will be arranged in a 3×3 array to obtain a similar active area as one of the $5.4 \times 5.4\,\mathrm{cm}^2$ detectors. For the TOF measurement the start timing detector will be a 3×3 array of $19 \times 19\,\mathrm{mm}^2$, 200 μm thick CVD (Chemical Vapour Deposition) polycrystalline Diamond detectors positioned 1 cm behind the secondary reaction target. Three different detector options are being considered for the stop timing measurement at the position of the LYCCA modules; a large area fast plastic scintillator, Diamond detectors or the DSSSD themselves.

8.2. Reaction: two-step fragmentation

One of the methods of radioactive ion beam production at HISPEC will be projectile fragmentation. Intermediate fragments will be separated using the FAIR/NuStAR fragment separator Super-FRS (Superconducting FRagment Separator) [16]. Although

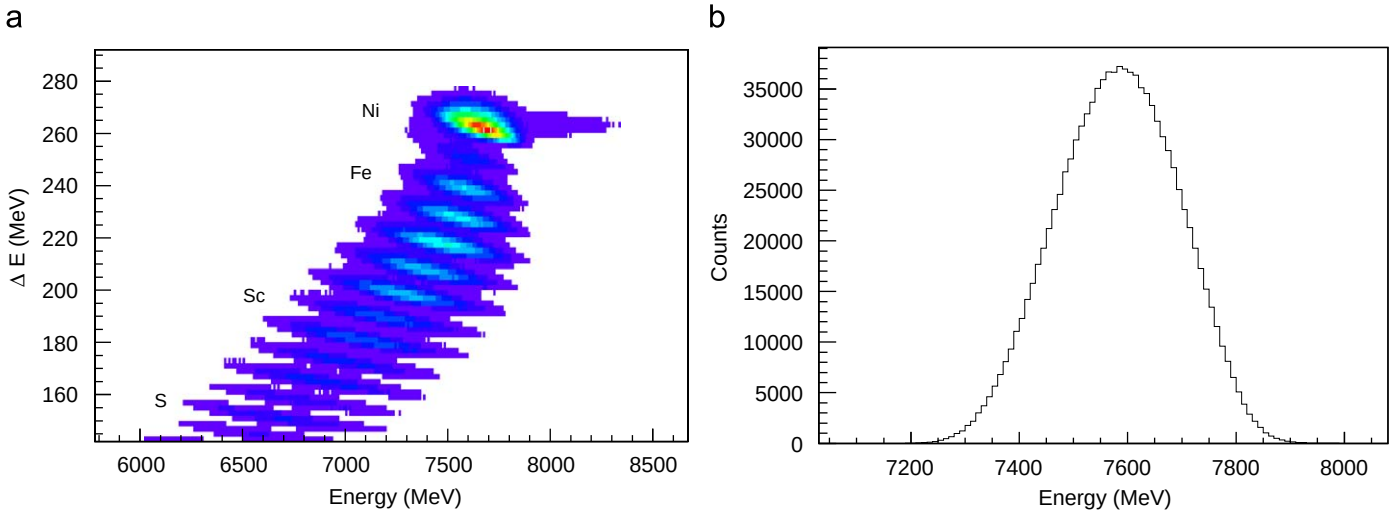

Fig. 3. (a) CATE ΔE versus E_t spectrum produced from data collected during a RISING fast beam campaign experiment to study ^{53}Ni. (b) Projection of (a) onto the total energy (x axis) for $Z = 26$ (Fe) fragments only. This spectrum clearly shows the limitation of the CATE detector system as the two isotopes of Fe with the largest production cross-sections (namely ^{52}Fe ($\sigma = 31.1$ mb) and ^{53}Fe ($\sigma = 52.8$ mb)) are not resolved.

the primary reaction before the Super-FRS may be of fragmentation type the second reaction to populate excited states in the nuclei of interest can take many forms including a second fragmentation reaction. The use of fragmentation reactions with RIBs poses many challenges, in particular the identification of the reaction products with broad energy and momentum distributions. The simulation is an ideal tool to investigate ion identification techniques with LYCCA-0 following two-step fragmentation reactions.

The sequence of reactions $^{58}\mathrm{Ni} + {}^{9}\mathrm{Be} \rightarrow {}^{55}\mathrm{Ni}$, $^{55}\mathrm{Ni} + {}^{9}\mathrm{Be} \rightarrow {}^{53}\mathrm{Ni}$ was chosen for the test case as real experimental data exist against which the simulation results can be compared. The data are from an experiment that was performed during the first RISING (Rare Isotope Spectroscopic INvestigation at GSI) [17] fast beam campaign to study the $T_z = -\frac{3}{2}$ nucleus ^{53}Ni [18–20]. A 600 MeV/u ^{58}Ni beam was incident on a 4 g/cm^2 ^{9}Be target and ^{55}Ni reaction products were tracked and separated by the existing GSI fragment separator FRS [21]. A range of intermediate fragments resulted from the primary reaction; however, for the simulated reaction an assumption has been made that in the analysis of real experimental data from fragment separator devices there would be unique identification of the intermediate fragments on an event-by-event basis. This was indeed achieved for the RISING experiment and thus the need to simulate reaction products other than ^{55}Ni was deemed unnecessary. The selected ^{55}Ni ions were then incident on another ^{9}Be target of thickness 700 mg/cm^2 where a second fragmentation reaction occurred. Again a large range of nuclei were produced following the secondary reaction along with the ^{53}Ni nuclei of interest. These secondary reaction products were identified using a combination of energy loss (Z) and total implantation energy (A) by the CATE (CAlorimeter TElescope) detector [22]. CATE measured fragment energy loss using an array of Si (ΔE) detectors and residual energy using an array of CsI (E_r) detectors located directly behind the Si. The intermediate fragment energy range for which the simulation package is applicable is dictated by the separating device being simulated. The FRS can analyse all ion beams of hydrogen through to uranium spanning energy ranges of 0.8–4.5 and 0.2–1.3 GeV/u, respectively [21].

Fig. 3a shows the ΔE versus E_t spectrum created from the CATE detector signals where $E_t = \Delta E + E_r$. Fig. 3a highlights the large range of secondary fragments produced and thus the need for good ion identification. Fig. 3a also shows that fragments with

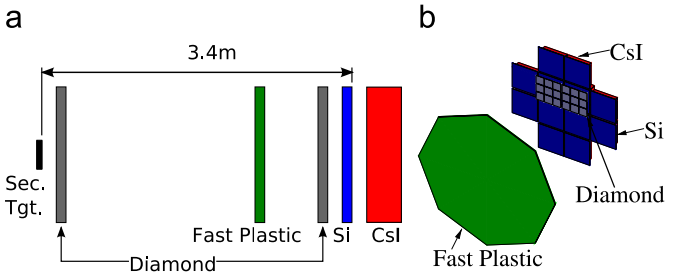

Fig. 4. (a) LYCCA-0 detector positions including the three stop timing options, fast plastic, Diamond and Si. (b) LYCCA-0 module geometries as viewed from the beam direction.

differing charge are fairly distinguishable. Fig. 3b shows the Fe gated projection of Fig. 3a onto the total energy (x) axis. As the total fragment energy is mass dependent, it was originally envisaged that the selection of a particular isotope, for prompt γ-ray correlations, would be possible from the measured total energy. However, Fig. 3b clearly shows that for this type of reaction and mass region, this was not possible with the CATE detector system. From this reaction the isotopes of Fe with the largest production cross-sections (calculated with EPAX2) are ^{52}Fe ($\sigma = 31.1$ mb) and ^{53}Fe ($\sigma = 52.8$ mb) which cannot be resolved in Fig. 3b. This is just one of the reasons behind the development of LYCCA: to achieve complete fragment identification in Z and A in order to produce clean γ-ray spectra for specific nuclei.

8.3. LYCCA-0 simulation

Fig. 4 shows the positions and geometries of the LYCCA-0 detector elements as defined in GEANT4. This version of the simulation incorporates the three different stop timing detector options, fast plastic, Diamond and Si and the LYCCA-0 modules are located such that the nominal secondary target-Si detector distance is 3.4 m.

The CsI detectors located behind the Si detectors are also shown. Only the active areas of the detectors are defined in the simulation, surrounding dead material such as PCB, wire bonds and holding frames are omitted. Also, ion channelling and incomplete charge collection are not simulated for the Si strip detectors. The detector materials are all defined as standard

nuclear physics solid state detector materials except for the Diamond detectors which have an increased carbon density of $3.5\,g/cm^3$, as per real CVD Diamond. The default resolutions imposed on the simulation detectors are summarised in Table 1 although these values can be modified interactively between each simulation run along with the target-detector module distance.

The definition of a 'good' event, within the simulation, is one that produces a start timing signal in the target position Diamond detectors, a stop timing signal in any one of the three stop timing detectors and ΔE, E_r signals in the Si and CsI detectors, respectively. This imposes a range of secondary fragment energies for which the simulation is applicable as the physics to be addressed requires the ions being studied to not only reach and deposit energy in the CsI detectors but also stop and not punch through. For the LYCCA-0 setup this energy range was determined for ^{12}C and ^{208}Pb fragments to be 20–105 and 55–445 MeV/u, respectively. If an event fulfils the 'good' event criteria the application reads in the corresponding intermediate fragment parameters and digitised FRS tracking detector signals are produced. All of the detector signals for 'good' events are passed to the *Analysis* module for storage and histogramming.

Table 1
Default full-width half-maximum (FWHM) values and units for the LYCCA-0 detector resolutions along with the acceptable ranges for the interactively changeable values.

Detector	Signal	Units	Range	Default value
Diamond	Energy	%	–[a]	1.0
	Time	ns	0–1000	0.05
Plastic	Energy	%	0–100	2.0
	Time	ns	0–1000	0.1
Si	Energy	%	0–100	1.0
	Time	ns	0–1000	0.2
CsI	Energy	%	0–100	0.5

[a] Not changed interactively.

9. Simulation results

This section will present some of the results from various investigations utilising the new simulation package for the reactions defined in Section 8.2 and the detector system defined in Section 8.1. For brevity the results shown use only the Diamond detectors for timing information and therefore the fast plastic detector was removed from the setup and the number of LYCCA-0 module Diamond detectors was increased to cover the same active area as the Si. Also, the final incarnation of the LYCCA detector system will incorporate only one type of timing detector and therefore the results presented here would have extra significance if Diamond was chosen.

9.1. $A \approx 50$

To truly validate simulation results, a comparison must be made with real experimental data. Fig. 5a shows, for comparison, the same CATE ΔE (Si) versus E_t (Si + CsI) plot as shown in Fig. 3a, along side Fig. 5b which is a similar plot created using the simulated LYCCA-0 Si and CsI detector signals. Unlike the simulated data the experimental data required a particle-γ coincidence condition which accounts for the difference in the relative fragment yields between the two plots. Also the Rutherford scattered ^{55}Ni intermediate fragments are not simulated but could be if required. The $A \approx 50$ event files were created using $\approx 1.1 \times 10^6$ primary beam particles which was the maximum number allowed for this reaction without exceeding the 2 GB file size limit. This resulted in $\approx 9.7 \times 10^5$ secondary events for a total of 91 fragment species with production

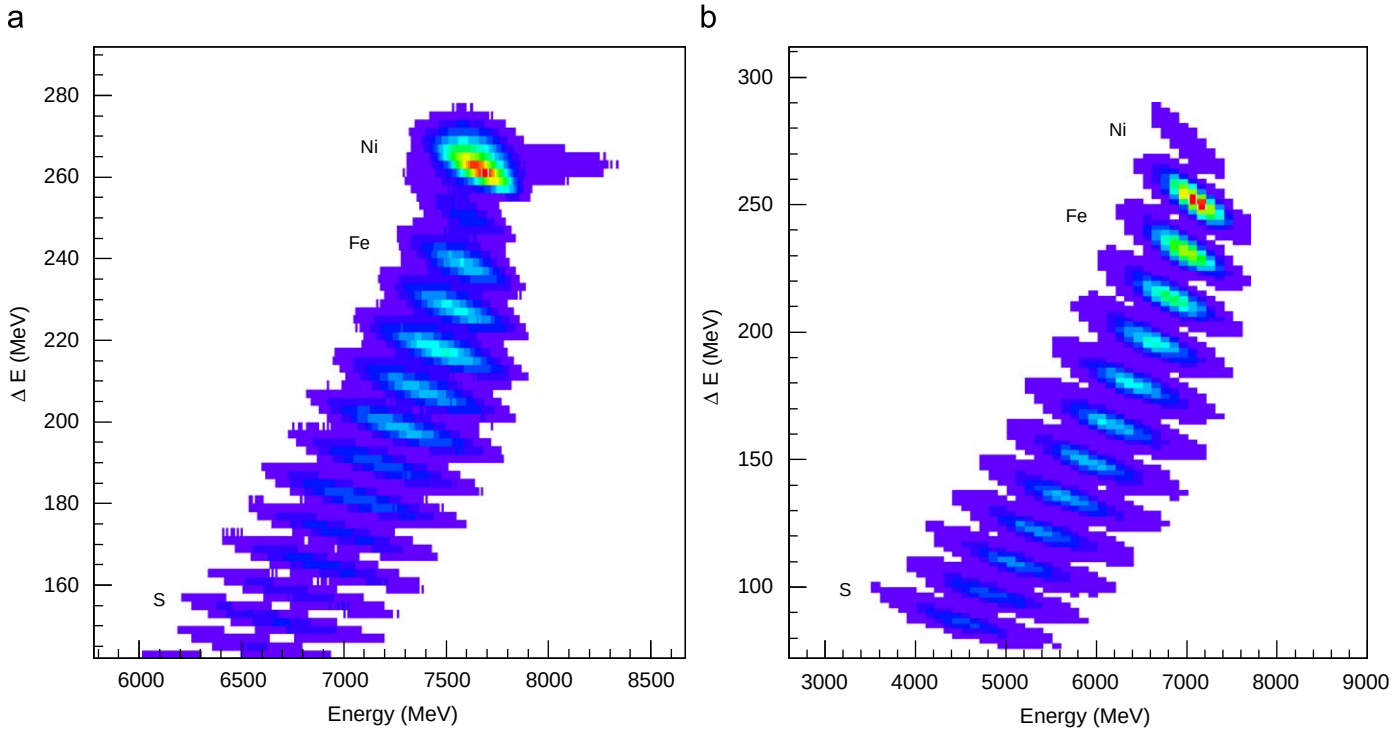

Fig. 5. (a) (same as in Fig. 3a) CATE ΔE versus E_t spectrum created with real experimental (particle-γ coincidence) data taken during the RISING ^{53}Ni experiment. (b) Simulated data, no particle-γ requirement and no Rutherford scattered ^{55}Ni fragments are simulated. The isotopes $^{53,54}Ni$, $^{49-53}Fe$ and $^{30-38}S$ were simulated for the labelled fragment species.

cross-sections $>1\,\mu b$. This yielded isotopes of ^{53,54}Ni, $^{49-53}$Fe and $^{30-38}$S for the fragment species labelled in Fig. 5. The simulation *system* runtime for these events was 45 s using a laptop PC with an Intel Pentium Centrino 2 GHz processor.

The primary purpose of the simulation of LYCCA-0 is to investigate fragment identification from energy and TOF measurements. Selecting $Z = 26$ (Fe) fragments a TOF versus energy (E_t) spectrum was produced using the start and stop timing signals from the CVD Diamond detectors. Fig. 6a shows the result of this analysis for a target-Si detector distance of 2 m (actual TOF path 1.98 m) and Fig. 6b for a distance of 3.4 m, the distance planned for LYCCA-0. Isotopic separation is clearly improved for the longer TOF path due to the fixed timing resolution (50 ps FWHM) of the Diamond detectors and four distinct regions can clearly be seen corresponding to the isotopes $^{50-53}$Fe. Figs. 6c and d show the same analysis but for sulphur isotopes. The isotopic separation is already very good at 2 m for the sulphur isotopes and becomes excellent when the distance is increased to 3.4 m. The separation improvement for low mass fragments over higher masses is predominantly due to the Si and CsI detector energy resolutions (1.0% and 0.5% FWHM, respectively) being a percentage of the measured energy. Hence the resolution decreases as the fragment mass increases.

An advantage of simulating detector systems is that acceptable detector properties, such as time resolution, can be investigated before any physical detectors are purchased. The simulation was used to determine the minimum acceptable resolution of the timing detectors for which clean fragment identification was possible using the proposed technique. Fig. 7a shows an Fe ($Z = 26$) gated, TOF versus E_t plot for a target-Si distance of 3.4 m but with a Diamond detector time resolution of 100 ps FWHM and Fig. 7b for 150 ps FWHM. Fe isotopic separation is just visible for the 100 ps case and disappears completely for 150 ps resolution. This analysis shows that a timing detector resolution of much less than 100 ps is required for $A \approx 50$ fragment identification using the TOF-ΔE–E_t technique with the Si, CsI energy resolutions unchanged.

9.2. Intermediate-secondary fragment correlations

The secondary fragment identification technique, as outlined in Section 8.1, requires the measurement of the fragment energy and TOF. Fig. 6 showed that isotopic separation (i.e. mass 'resolution') became less pronounced as the fragment mass increased and the TOF path decreased, also Fig. 7 showed a deterioration as the timing detector resolution decreased. To address these technique limitations, an investigation into the possibility of mass resolution improvement through correlations with the intermediate fragments was performed. The simulation allows the user to investigate correlations between the LYCCA-0 and the FRS tracking detector signals. As the intermediate fragments pass through the FRS, (x, y) position information from multiwire proportional counters, timing from scintillation detec-

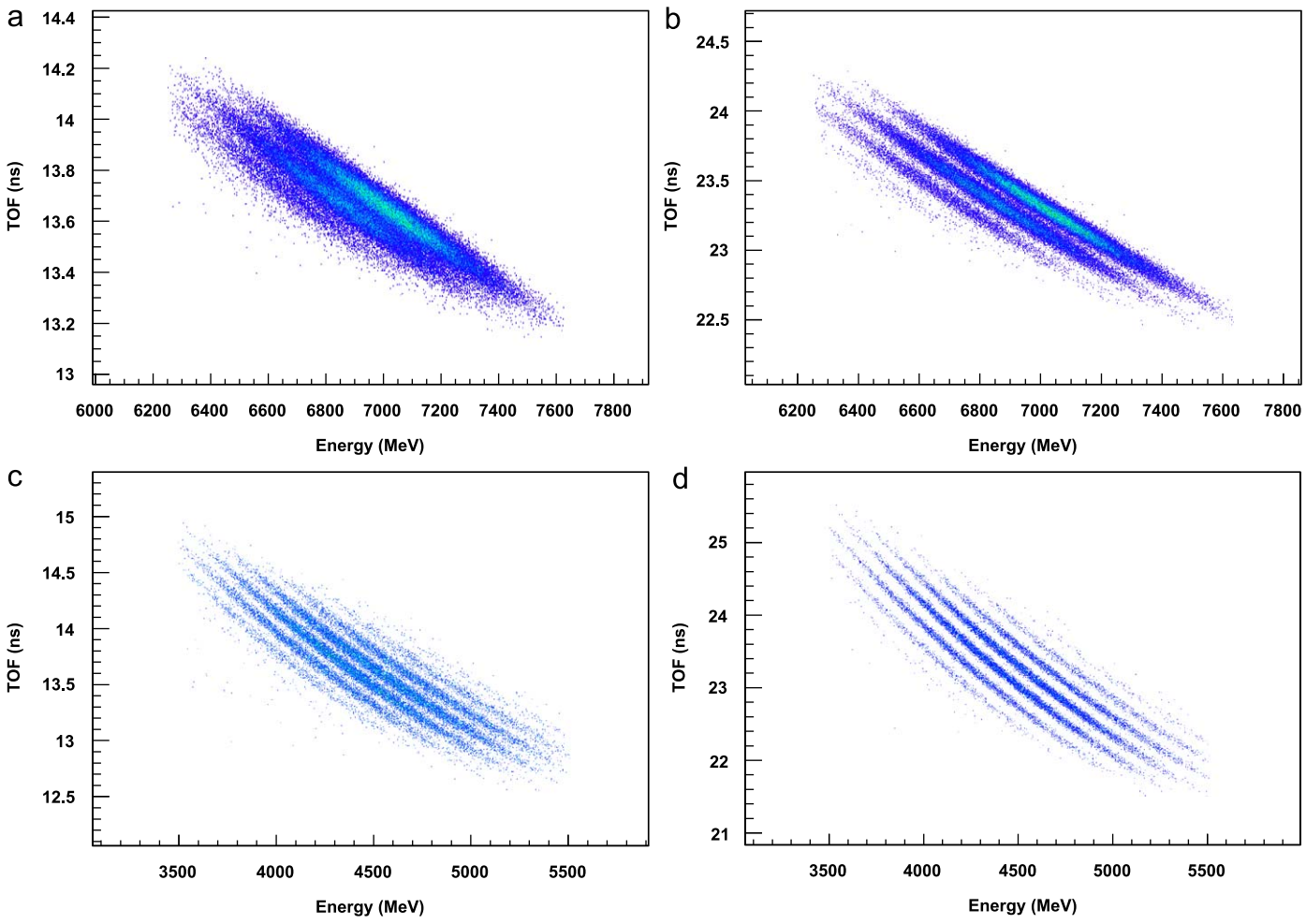

Fig. 6. Simulation results: TOF versus energy (E_t) spectra for two fragment types and two target-Si detector distances. (a) Fe and 2 m, (b) Fe and 3.4 m, (c) S and 2 m and (d) S and 3.4 m.

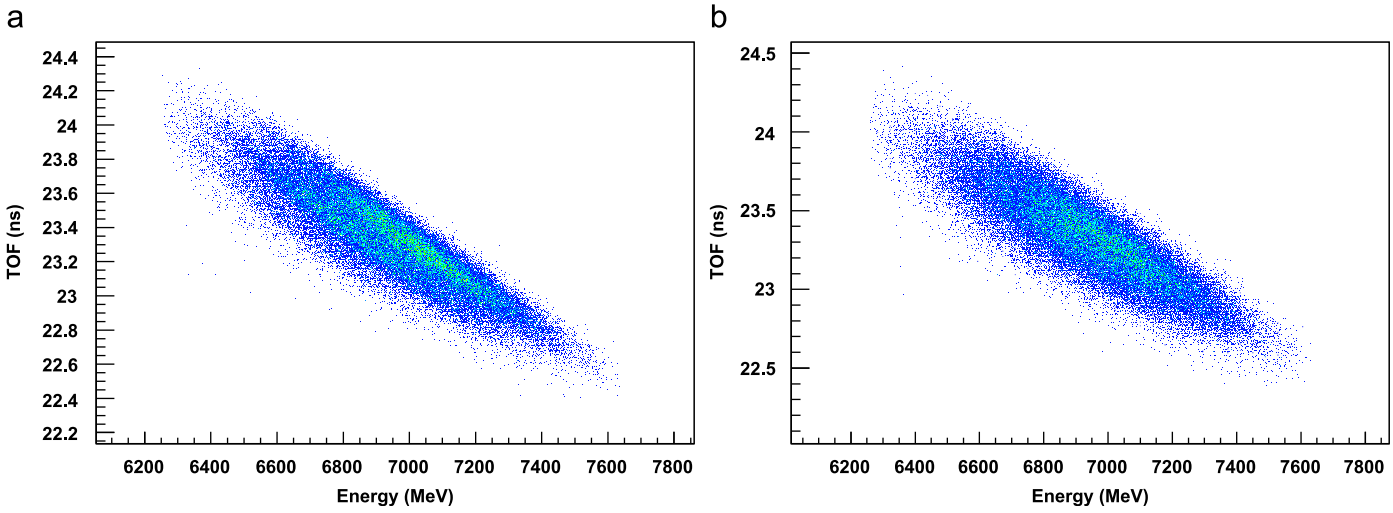

Fig. 7. TOF versus E_t spectra for $^{49-53}$Fe fragments with Diamond timing detector resolutions of (a) 100 ps and (b) 150 ps.

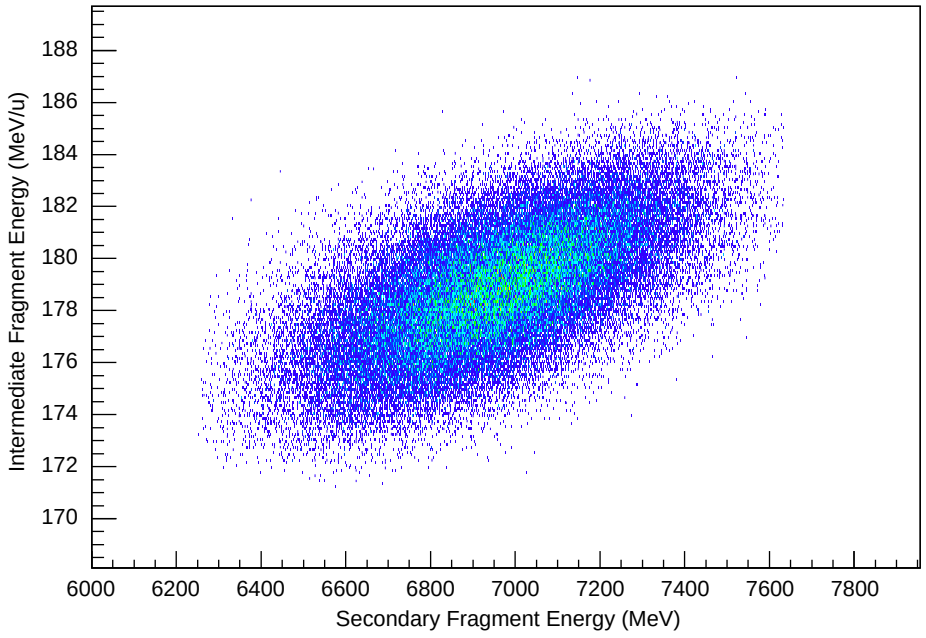

Fig. 8. Intermediate fragment energy just before the second reaction target plotted against the secondary fragment energy (E_t), as measured by the LYCCA-0 Si and CsI detectors, for Fe secondary fragments. As the energy of the fragment is used to determine its mass, this correlation gives another observable to aid fragment identification.

tors and energy loss from an ionisation chamber are all recorded. Within the simulation, the user can also access particle characteristics at any position in the experimental setup without the need for a virtual detector at that position. For example, the energy of a ^{55}Ni intermediate fragment can be accessed immediately before the second reaction target.

Firstly, the intermediate fragment energies were plotted against E_t for Fe secondary fragments to ascertain whether a correlation exists. The result of this analysis is shown in Fig. 8 where a definite correlation between the two quantities can be seen.

Fig. 9a shows the intermediate fragment energy, taken directly before the second reaction target, plotted against the Fe secondary fragments mass which is calculated from energy and TOF as measured by the LYCCA-0 CsI and Diamond detectors, respectively. Fig. 9b shows a projection of 9a onto the mass (x) axis. Although distinct peaks relating to the different Fe fragment masses can be seen in Fig. 9b, Fig. 9a shows that this spectrum could clearly be improved if the semi-major axes of the distributions were all vertical. It is also important to note that the calculated fragment mass numbers (A) are incorrect as the largest distribution should result from ^{53}Fe fragments. The observed correlation and incorrect mass numbers in Fig. 9 are due to the exclusion of the energy lost in the timing and Si detectors situated in the fragments flight path. For the best possible fragment mass identification, using only information gained from the LYCCA-0 detectors, an accurate measurement of the fragments total energy is required. In reality the energy resolution of the Diamond and Si detectors may be significantly different from that estimated for such high energy fragments. If this is the case, the measured energy loss in these detectors, when included in the mass calculation for Fig. 9, may not result in any significant improvement in mass separation. Also, the final LYCCA-0 detectors will be chosen and tailored for specific measurements. For example, the TOF detectors will be chosen purely on the basis of timing characteristics, not energy resolution, and therefore only

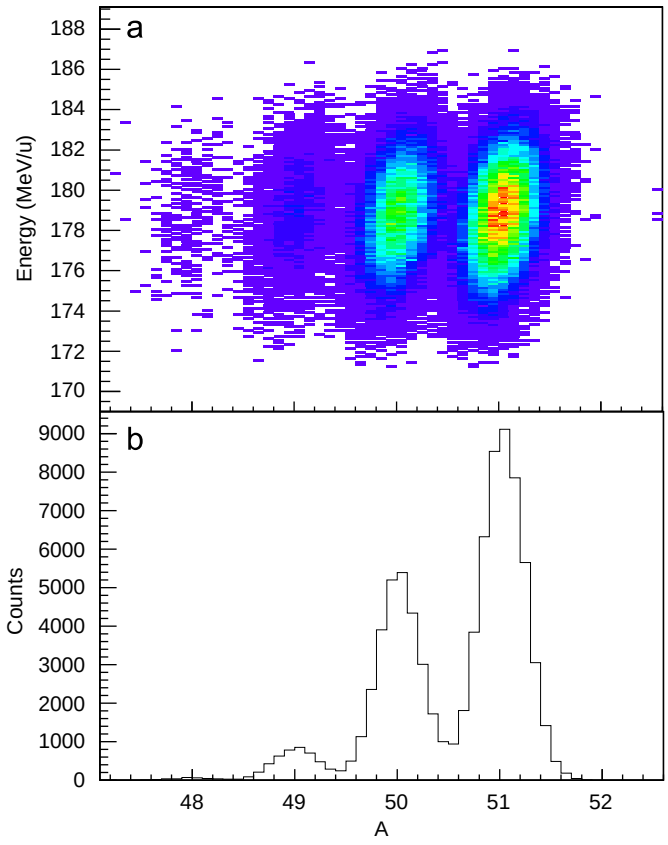

Fig. 9. (a) Intermediate fragment energy immediately before the second reaction target plotted against the secondary fragment mass calculated from the fragments TOF and energy as measured by the Diamond and CsI detectors, respectively. (b) Total projection of (a) onto the mass (x) axis.

timing signals may be collected from these detectors. In fact, it may be that calculating the energy loss in the timing and Si detectors yields far less uncertainty than actual measurement. It may be possible to improve Fig. 9b with the incorporation of the calculated energy loss in each detector determined by the fragments flight path. The fragment trajectory would be deduced from the segmentation and position sensitivity of the detectors. These calculations and analysis are beyond the scope of this article, but they demonstrate effectively how the simulation may be used to determine the optimum experimental configuration and analysis methodology. Fig. 9 ultimately shows that fragment mass resolution could be improved with the accurate knowledge of either the intermediate or the secondary fragment energy along with the measured TOF across the LYCCA-0 detectors.

9.3. $A \approx 100$

Experiments performed at HISPEC would not be limited to nuclei with $A \approx 50$ or less and therefore determining the validity of the identification technique for higher mass fragments is crucial. The simulation is ideally suited for this and can help to establish any limitations by simulating a variety of experiments with the nuclei of interest covering a large mass and energy range. A two-step fragmentation reaction was simulated to produce nuclei in the $A \approx 100$ region. A primary beam of ^{112}Sn at 635 MeV was used to produce ^{110}Sn intermediate fragments which were then used to produce $^{104-107}$Cd secondary fragments. The reaction targets, FRS tracking detectors and LYCCA-0 detector system remained unchanged from the Ni reaction.

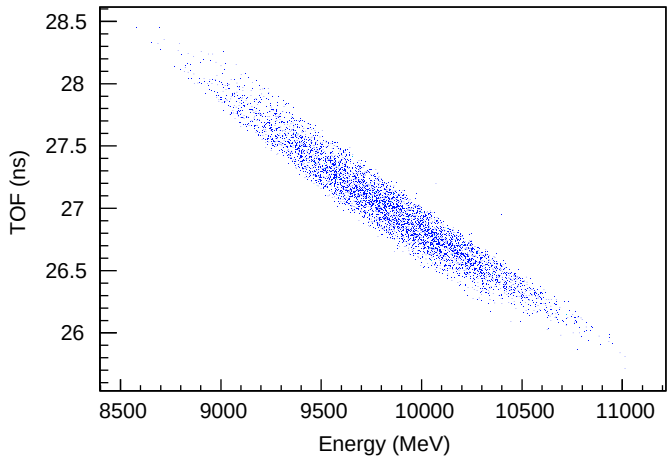

Fig. 10. TOF versus E_t spectrum for Cd fragments, produced in the simulated ^{112}Sn → ^{110}Sn → $^{104-107}$Cd reaction, with a target-Si detector distance of 3.4 m.

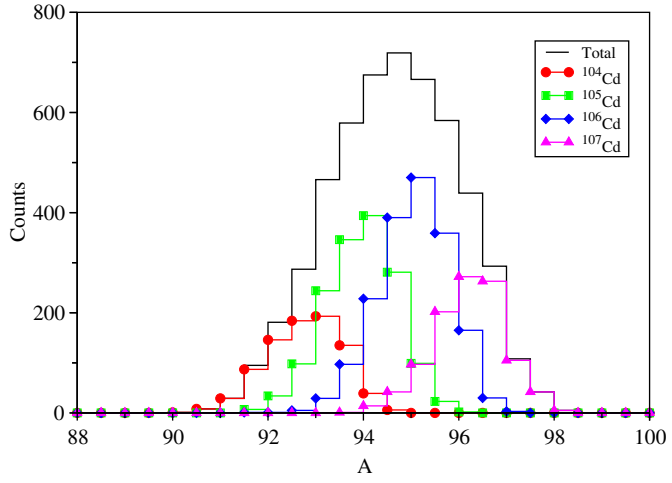

Fig. 11. Calculated mass distributions from TOF and energy (E_r) measurements for the $^{104-107}$Cd fragments along with their summation.

Fig. 10 shows the result of plotting the TOF versus E_t for the Cd reaction, for a target-Si detector distance of 3.4 m. The detector resolutions imposed for this analysis are as per Table 1 and the plot does not show clear isotopic separation for the Cd isotopes.

Fig. 11 shows the calculated mass distributions for the Cd isotopes from TOF (Diamond) and energy (CsI only) measurements. Although the centroids of the individual mass distributions are separated the resolution is of the order of three mass units and therefore the clean selection of a particular isotope would be extremely difficult without contamination from neighbouring isotopes. This analysis starts to highlight the limitations of the fragment identification technique with the described setup for experiments involving $A \approx 100$ fragments and indicates that for this mass region, additional selection devices are likely to be required.

10. Summary

A new simulation package has been developed which utilises the ion transport code MOCADI to generate parameters describing realistic ions following a fragmentation reaction which are tracked through a separator device. The output from MOCADI is modified into a format which can then be read by the next stage of the simulation which is an application written using the GEANT4 framework. The secondary fragments are tracked through the virtual

detector system and parameters such as energy loss, interaction position and time are digitised and passed to an analysis module. The simulation uses the data analysis software ROOT to histogram and store the digitised detector signals. This allows the user to perform data analysis on the simulated data in much the same way as one would with real experimental data. The simulation has been used to successfully model a new detector system prototype, LYCCA-0, which in the first instance will be used to identify reaction products following two-step fragmentation reactions. The results from this have been used to validate an ion identification technique which uses fragment time-of-flight and energy as measured by LYCCA-0 modules. The simulation package can presently be downloaded via the LYCCA web page: http://www.nsg.nuclear.lu.se/lycca/.

Acknowledgements

The authors wish to thank Helmut Weick for his help with certain aspects of MOCADI and the RISING collaboration for their contribution during the collection of the ^{53}Ni data. MJT and MAB would also like to acknowledge financial support for this work from the Engineering and Physical Sciences Research Council (EPSRC) and the Science and Technology Facilities Council (STFC).

References

[1] J.J. Gaimard, K-H. Schmidt, Nucl. Phys. A 531 (1991) 709.
[2] K. Sümmerer, B. Blank, Phys. Rev. C 61 (2000) 034607.
[3] T. Czosnyka, et al., Nucl. Phys. A 458 (1986) 123.
[4] H. Ower, Computer Program CLX.
[5] N. Iwasa, et al., Nucl. Instr. and Meth. B 126 (1997) 284.
[6] D. Bazin, et al., Nucl. Instr. and Meth. A 482 (2002) 307.
[7] O. Tarasov, D. Bazin, Nucl. Phys. A 746 (2004) 411.
[8] Geant4 Collaboration, Nucl. Instr. and Meth. A 506 (2003) 250.
[9] X-5 Monte Carlo Team, Los Alamos National Laboratory, Los Alamos, USA, April 2003.
[10] A.S. Goldhaber, Phys. Lett. B 53 (1974) 306.
[11] R. Brun, F. Rademakers, Nucl. Instr. and Meth. A 389 (1997) 81 (see also ⟨http://root.cern.ch/⟩).
[12] LYCCA Homepage, ⟨http://www.nsg.nuclear.lu.se/lycca/⟩.
[13] HISPEC Homepage, ⟨http://www.gsi.de/fair/experiments/NUSTAR/hispec_e.html⟩.
[14] NuStAR Collaboration Homepage, ⟨http://www.gsi.de/fair/experiments/NUSTAR/index_e.html⟩.
[15] FAIR Facility Homepage, ⟨http://www.gsi.de/fair/index_e.html⟩.
[16] H. Geissel, et al., Nucl. Instr. and Meth. B 204 (2003) 71.
[17] H.J. Wollersheim, et al., Nucl. Instr. and Meth. A 537 (2005) 637.
[18] M.J. Taylor, et al., J. Phys. G Nucl. Part. Phys. 31 (2005) S1527.
[19] G. Hammond, et al., Acta Phys. Pol. B 36 (2005) 1253.
[20] G. Hammond, Ph.D. Thesis, University of Keele, 2008.
[21] H. Geissel, et al., Nucl. Instr. and Meth. B 70 (1992) 286.
[22] R. Lozeva, et al., Nucl. Instr. and Meth. A 562 (2006) 298.